Supporting Information for

Exploring a wider range of Mg-Ca-Zn metallic glass as biocompatible alloys using combinatorial sputtering

Jinyang Li, Forrest S. Gittleson, Yanhui Liu, Jingbei Liu, Ayomiposi Michelle Loye, Lyndsey McMillon-Brown, Themis R. Kyriakides, Jan Schroers, and André D. Taylor*

**Department of Chemical and Environmental Engineering, Yale University, 9 Hillhouse Avenue, New Haven, CT, United States. E-mail: andre.taylor@yale.edu*

Experimental

1. Materials and Methods

1.1 Material Synthesis and Characterization

Mg-Ca-Zn metallic glass thin film samples, about 1μm in thickness, were deposited from high purity metal targets (99.99%) on a 4 inch silicon wafer with a conducting layer of Cr beneath by a co-sputtering system reported previously,[1] as illustrated in Figure 1a. The composition, measured by energy-dispersive X-ray spectroscopy (EDS), of each sample in the sputtered library of Mg-Ca-Zn samples varied as a function of substrate-to-target orientation and distance. The sample area was precisely confined using a shadow mask with arrays of 0.83 cm^2 open circles. The film microstructure was characterized by scanning electron microscopy (SEM) (Hitachi SU-70) and crystallinity was evaluated by X-ray diffraction (XRD) (Rigaku) with a Cu Kα radiation source. Simulated body fluid (SBF) was prepared with the following composition from Milli-Q water: 142.0 mM Na^+, 5.0 mM K^+, 1.5 mM Ca^{2+}, 2.5 mM Mg^{2+}, 147.8 mM Cl^-, 4.2 mM HCO_3^-, 0.5 mM SO_4^{2-}, 1.0 mM HPO_4^{2-}.

1.2 Electrochemical Measurement

The microstructure of Mg-Ca-Zn metallic glasses selected from the sputtered thin films was characterized before and after electrochemical characterization in SBF by SEM. Electrochemical measurements were conducted with a three-electrode setup comprising a Pt mesh counter electrode, an Ag/AgCl reference electrode and a jacketed reactor with a Pt-wire attached O-ring for a leak-free connection to the silicon wafer sample library, as shown in Fig. 1. The exposed area are slightly larger than that of the masked metallic glass thin film to ensure complete utilization. Besides, there are no signs of corrosion behavior when testing on the conducting Cr layer by itself and therefore only the masked metallic thin films are tested. Each alloy sample was evaluated separately with fresh SBF electrolyte at 37 (± 0.5) °C. The open circuit potential (OCP) test would help find the voltage range during the sweeping in the polarization. However, given the small thickness of the thin films, it is not feasible to apply general OCP tests like the bulk specimen. Based on literature, we speculate the sweeping range for these metallic glass thin films. Voltammograms were acquired at a scan rate of 1 mV/s from -2.1 V to -0.6 V vs. Ag/AgCl using a Bio-Logic VMP3 potentiostat. Such a high scan rate again is to accommodate the small thickness of the thin films. The corrosion potentials (V_{corr}) and currents (i_{corr}) were calculated via linear fit and Tafel

extrapolation, where the intersection of anodic and cathodic Tafel lines produced values of V_{corr} and i_{corr}. We estimate the error in deriving V_{corr} and i_{corr} from Tafel extrapolation to be < 5 %.

1.3 Indirect cytotoxicity assay

Human osteosarcoma cells (MG63, ATCC) were maintained in Minimal Essential Medium Alpha (MEM, alpha), 10% Fetal Bovine Serum (FBS) and 1% penicillin-streptomycin at 37°C in a humidified atmosphere of 5% CO2. MG63 cells were cultured at 10,000 cells per well in a 96 well plate for 24 hours to allow attachment. The exposed area of metallic glasses was isolated using a cloning ring and 300µl of serum free MEM alpha incubated on the samples at 37°C and 5% CO2 for 24 hours. The extraction media was collected and 100µl of this volume was added to attached cells for 24 hours. Cells maintained in serum-free MEM were used as a positive control. Cell viability was assayed using a live/dead assay (Invitrogen). Media was removed and cells were stained with calcein-AM (live-green) and ethidium homodimer-1 (dead-red) for 10 mins, and imaged using a Zeiss fluorescent microscope. Live and dead cells were quantified using ImageJ with percent viability defined as the number of live cells divided by total cells attached multiplied by 100.

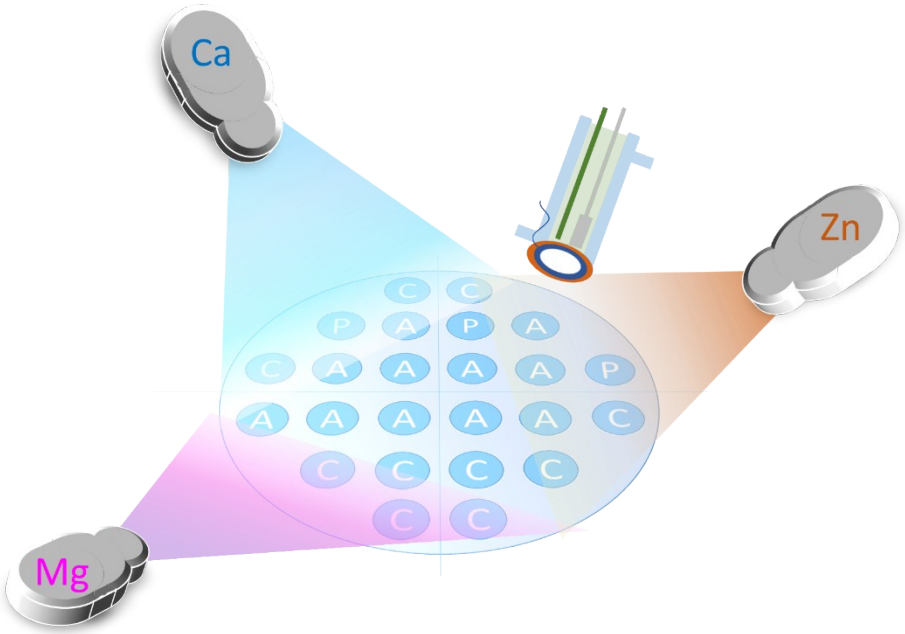

Scheme S1. Illustration of co-sputtered metallic glass thin films under three sputtering metal target, with letter A representing amorphous, C representing crystalline and P representing partly amorphous. The electrochemical setup is composed of a Pt wire (dark blue) attached O-ring (orange), a Pt mesh (silver) and a reference electrode (dark green) in a jacket reactor (light blue).

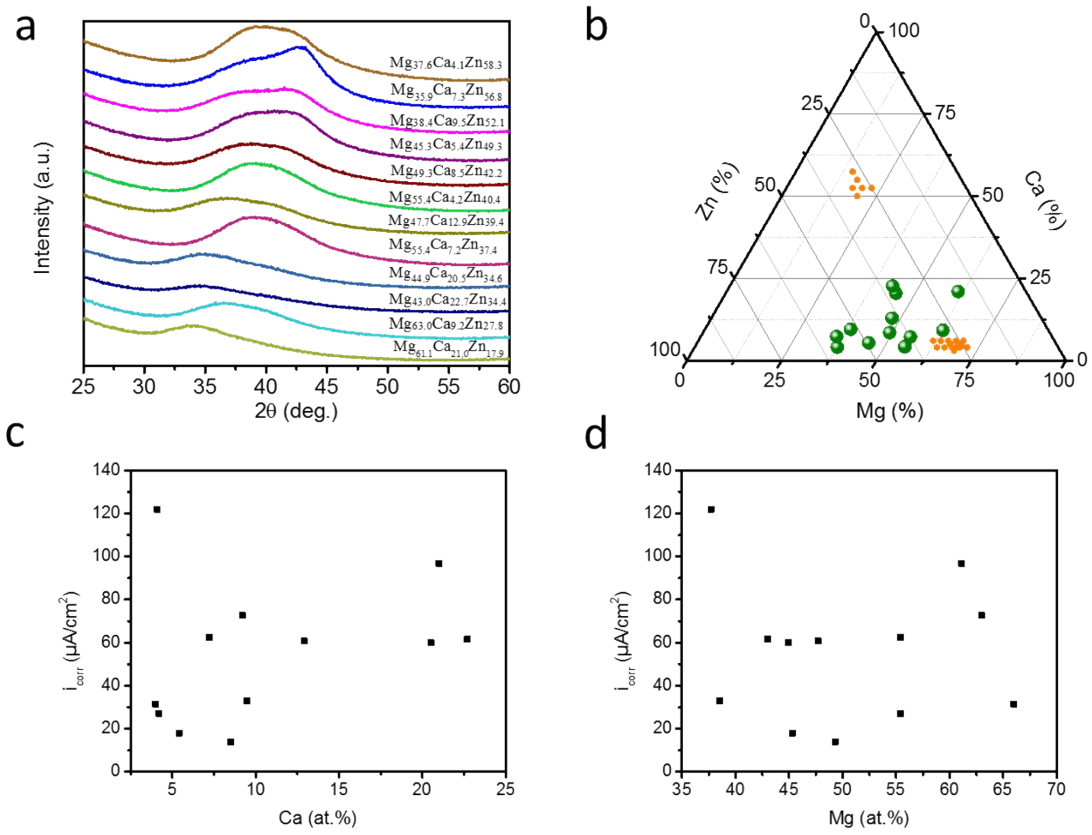

Scheme S2. (a) XRD patterns of co-sputtered metallic glasses samples with a decreasing Zn content order from top to bottom. (b) Triangle plot of compositions reported in this work (green dots) and other work (orange dots). Corrosion current i_{corr} versus (c) Ca and (d) Mg

Table S1 Corrosion potential (Vcorr), corrosion current (icorr) and composition before and after polarization measured by EDX of Mg-Ca-Zn metallic glasses in order of decreasing Zn content.

Initial Composition	Final Composition	E_{corr} vs. Ag/Ag Cl (V)	i_{corr} ($\mu A/cm^2$)
$Mg_{37.6}Ca_{4.1}Zn_{58.3}$	$Mg_{22.7}Ca_{3.2}Zn_{74.1}$	-1.347	121.9
$Mg_{35.9}Ca_{7.3}Zn_{56.8}$	$Mg_{11.6}Ca_{6.5}Zn_{81.9}$	-1.372	98.86
$Mg_{38.4}Ca_{9.5}Zn_{52.1}$	$Mg_{9.1}Ca_{7.0}Zn_{83.9}$	-1.119	32.96
$Mg_{45.3}Ca_{5.4}Zn_{49.3}$	$Mg_{11.7}Ca_{5.6}Zn_{82.7}$	-1.257	17.95
$Mg_{49.3}Ca_{8.5}Zn_{42.2}$	$Mg_{22.5}Ca_{6.9}Zn_{70.6}$	-1.224	13.93
$Mg_{55.4}Ca_{4.2}Zn_{40.4}$	$Mg_{20.5}Ca_{3.5}Zn_{76.0}$	-1.264	27.16
$Mg_{47.7}Ca_{12.9}Zn_{39.4}$	$Mg_{12.4}Ca_{7.1}Zn_{80.5}$	-1.296	60.67
$Mg_{55.4}Ca_{7.2}Zn_{37.4}$	$Mg_{21.4}Ca_{5.7}Zn_{72.9}$	-1.328	62.37
$Mg_{44.9}Ca_{20.5}Zn_{34.6}$	$Mg_{23.6}Ca_{10.9}Zn_{65.5}$	-1.421	59.98
$Mg_{43.0}Ca_{22.7}Zn_{34.3}$	$Mg_{22.3}Ca_{14.5}Zn_{63.2}$	-1.432	61.52
$Mg_{63.0}Ca_{9.2}Zn_{27.8}$	$Mg_{30.1}Ca_{7.7}Zn_{62.2}$	-1.395	72.61
$Mg_{61.1}Ca_{21.0}Zn_{17.9}$	$Mg_{8.2}Ca_{10.2}Zn_{81.6}$	-1.446	96.83
Mg	-	-1.636	147.91

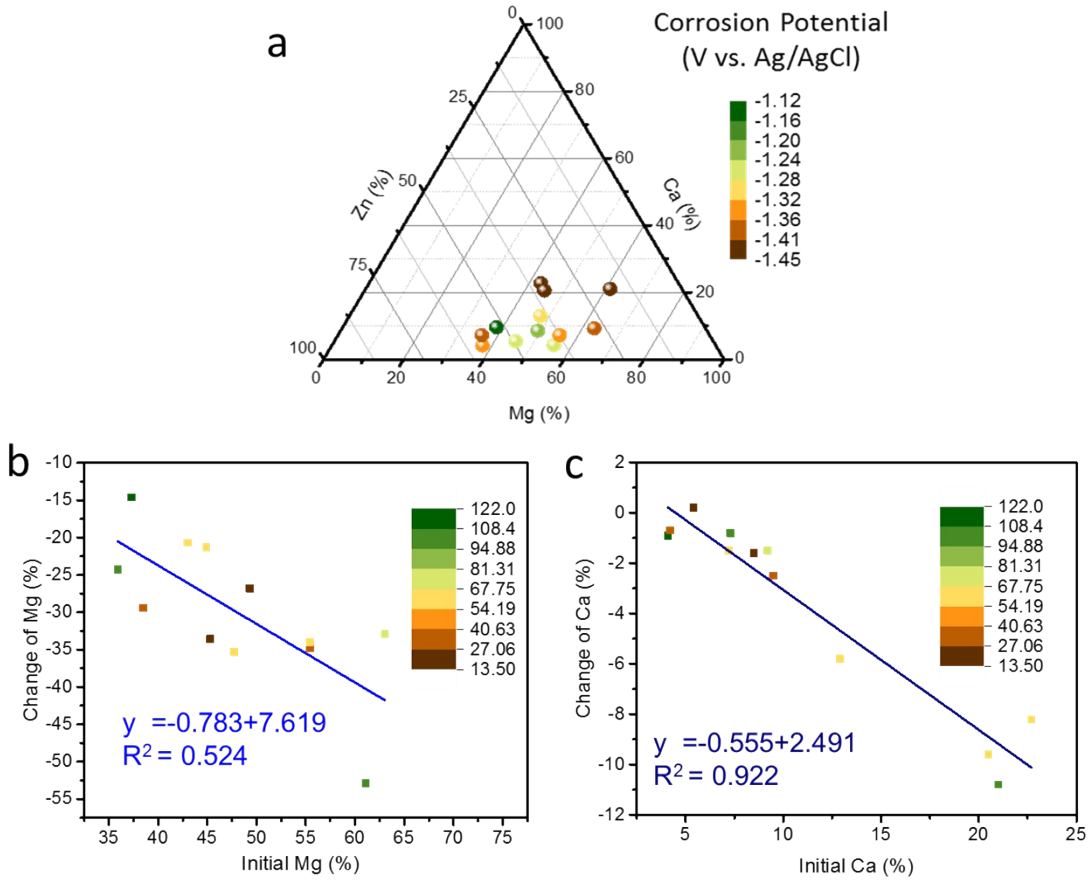

Scheme S3. (a) Ternary compositional mapping with the color code of corrosion potential V_{corr}. Change of element versus initial element content of c) Mg and d) Ca.

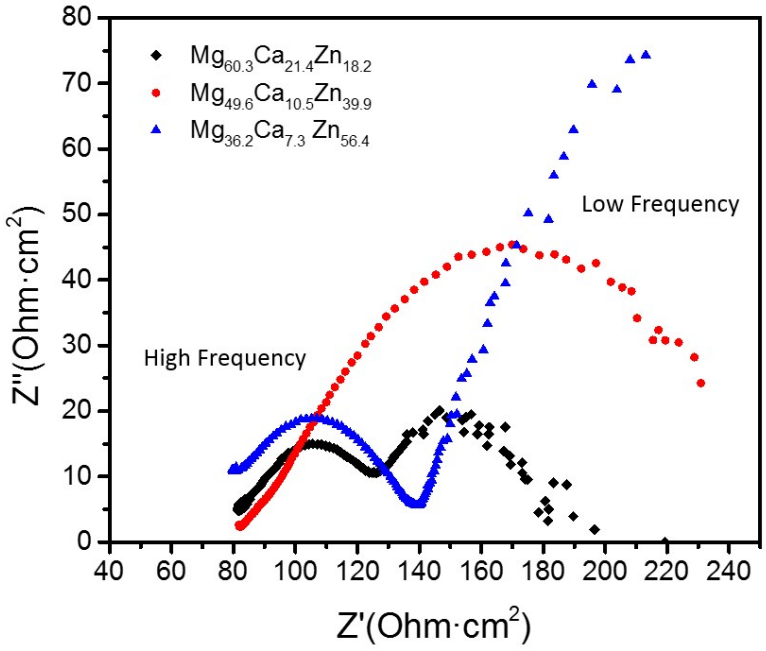

Scheme S4. Nyquist plot of $Mg_{60.3}Ca_{21.4}Zn_{18.2}$, $Mg_{49.6}Ca_{10.5}Zn_{39.9}$, $Mg_{36.2}Ca_{7.3}Zn_{56.4}$.

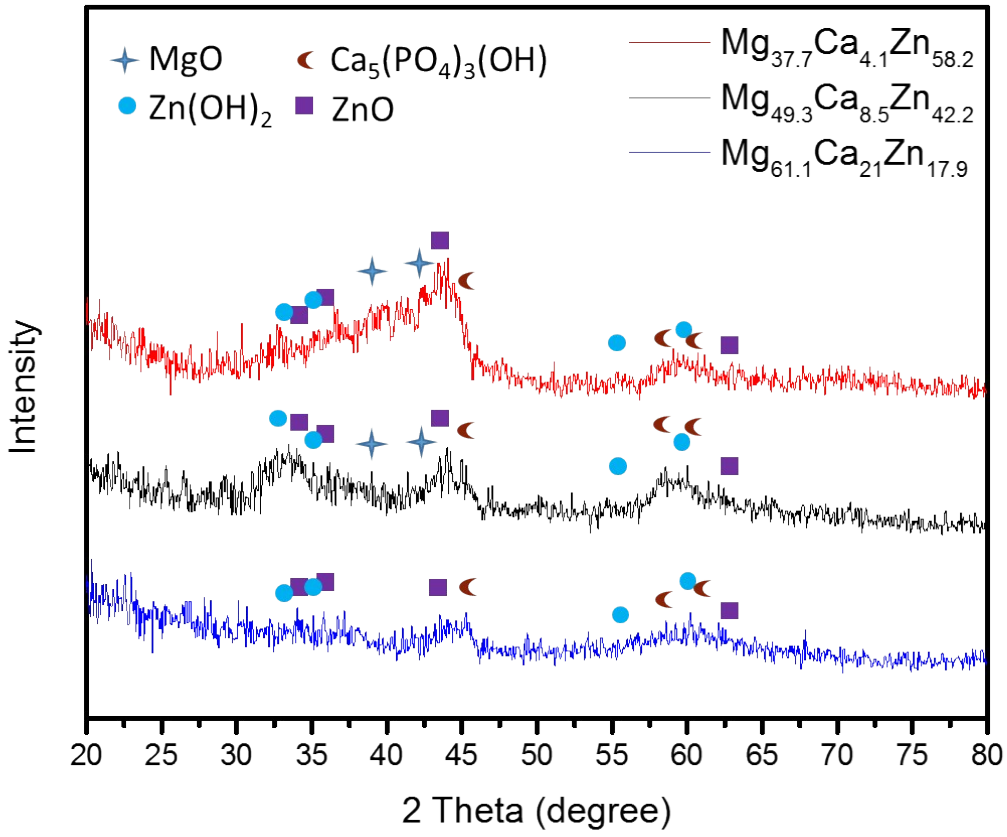

Scheme S5. XRD patterns of selected metallic glasses samples with various Zn content, i.e. $Mg_{37.7}Ca_{4.1}Zn_{58.3}$, $Mg_{49.3}Ca_{8.5}Zn_{42.2}$, and $Mg_{61.1}Ca_{21.0}Zn_{17.9}$ after the polarization in SBF at 37 (± 0.5) °C.

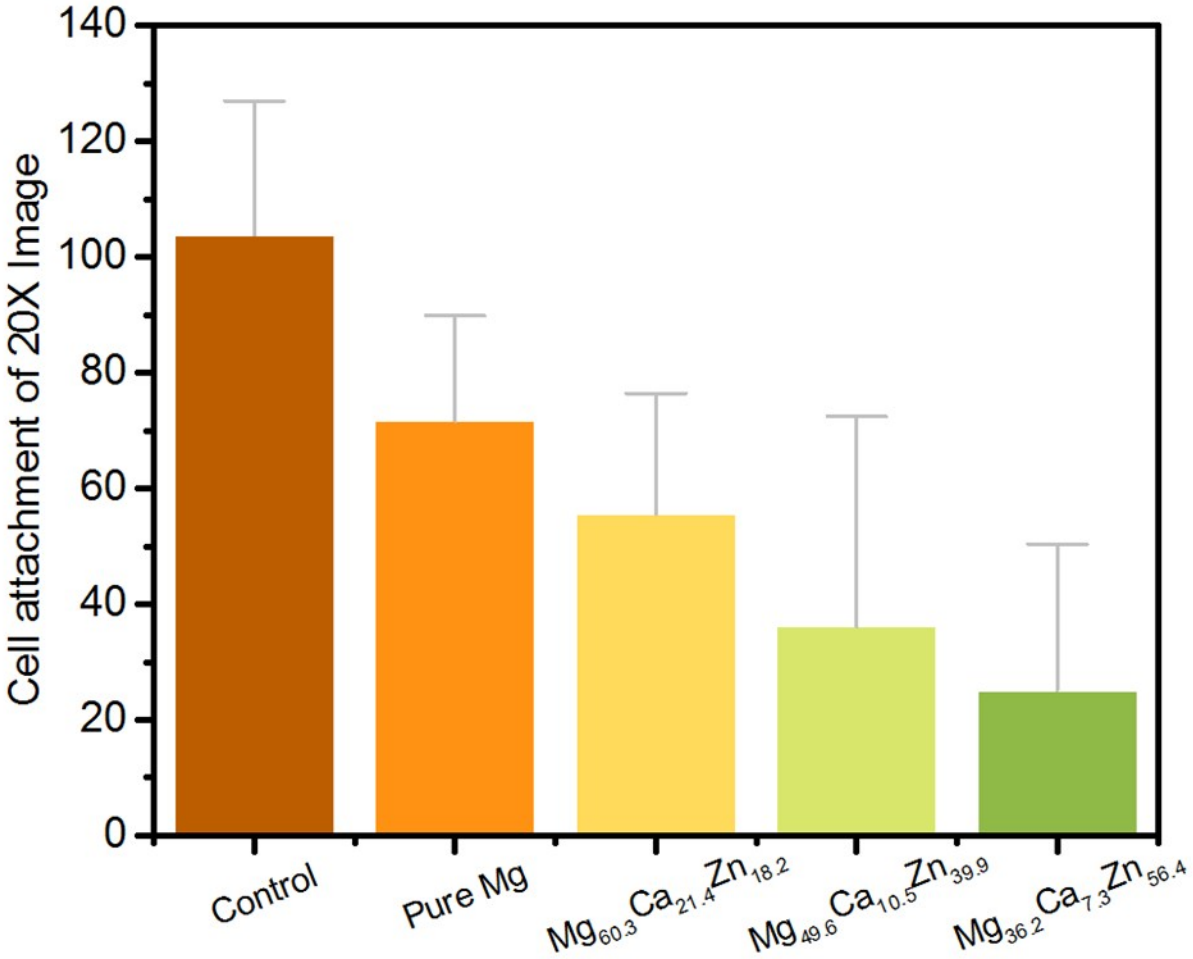

Scheme S6. Cell attachment in 20X image of control group (without metallic samples) and selected metallic glasses samples in the order of increasing Zn content, i.e. $Mg_{60.3}Ca_{21.4}Zn_{18.2}$, $Mg_{49.6}Ca_{10.5}Zn_{39.9}$, $Mg_{36.2}Ca_{7.3}Zn_{56.4}$ after 24 hours of incubation in the indirect cytotoxicity assay, using a Zeiss fluorescent microscope. The error bar represents the standard deviation, n =3.

References

[1] Y. Liu, J. Liu, S. Sohn, Y. Li, J.J. Cha, J. Schroers, Metallic glass nanostructures of tunable shape and composition, Nature Communications, 6 (2015) 7043.